

An Optimized Individual Target Brain in the Talairach Coordinate System¹

P. Kochunov,* J. Lancaster,*² P. Thompson,† A. W. Toga,† P. Brewer,* J. Hardies,* and P. Fox*

*Research Imaging Center, University of Texas Health Science Center at San Antonio, San Antonio, Texas 78284; and

†Laboratory of Neuro Imaging, Department of Neurology, UCLA School of Medicine, Los Angeles, California 90024

Received August 3, 2001

The goal of regional spatial normalization is to remove anatomical differences between individual three-dimensional brain images by warping them to match features of a single target brain. Current target brains are either an average, suitable for low-resolution brain mapping studies, or a single brain. While a single high-resolution target brain is desirable to match anatomical detail, it can lead to bias in anatomical studies. An optimization method to reduce the individual anatomical bias of the ICBM high-resolution brain template (HRBT), a high-resolution MRI target brain image used in many laboratories, is presented. The HRBT was warped to all images in a group of 27 normal subjects. Displacement fields were averaged to calculate the “minimal deformation target” (MDT) transformation for optimization. The greatest anatomical changes in the HRBT, following optimization, were observed in the superior precentral and postcentral gyri on the right, the right inferior occipital, the right posterior temporal lobes, and the lateral ventricles. Compared with the original HRBT, the optimized HRBT showed better anatomical matching to the group of 27 brains. This was quantified by the improvements in spatial cross-correlation and between the group of brains and the optimized HRBT ($P < 0.05$). An intended use of this processing is to create a digital volumetric atlas that represents anatomy of a normal adult brain by optimizing the HRBT to the group consisting of 100+ normal subjects. © 2002

Elsevier Science (USA)

INTRODUCTION

Spatial normalization (SN) refers to a class of image-processing algorithms that reduce interindividual anatomical variance by matching homologous spatial features of a “source” brain to those of a “target” brain.

¹ Research support was provided by the Human Brain Mapping Project, which is jointly funded by NIMH and NIDA (P20 MH/DA52176).

² To whom correspondence and reprint requests should be addressed. Fax: (210) 567-8152. E-mail: JLANCASTER@uthscsa.edu.

Spatial normalization can be broadly classified as global or regional. Global normalization uses a parametric description of the whole brain (position, orientation, and dimensions) to perform affine transformations, with up to 12 parameters, although in most instances of global normalization, only 9 parameters are used (three each for rotation, translation, and scaling) (Fox *et al.*, 1985; Fox, 1995; Collins *et al.*, 1995; Woods *et al.*, 1993; Woods, 1996; Lancaster *et al.*, 1995, 1999; Ashburner and Friston, 1997).

The goal of regional spatial normalization is to remove anatomical differences between individual three-dimensional (3-D) brain images at varying scales, down to the limiting resolution of 3-D MR brain images, by warping them to match features of a single target brain. A new regional spatial normalization algorithm called octree spatial normalization (OSN) was proposed in Kochunov *et al.* (1999). OSN reduced processing time from hours to minutes while approaching the accuracy of previous methods (Miller *et al.*, 1993; Collins *et al.*, 1995; Ashburner and Friston, 1999). The modifications of the OSN algorithm for use in human brain images were described and tested in Kochunov *et al.* (2000). There, the anatomical landmark-matching capability of OSN was evaluated with several major sulci (precentral, central, and postcentral sulcus and Sylvian fissure). This work showed that OSN significantly reduced intersubject anatomical variability relative to a global transform in every sulcus studied.

With the advent of fast high-quality regional spatial normalization methods such as OSN, research efforts now focus on better target brains. The target brains currently used are either an intensity-averaged brain, suitable for low-resolution brain-mapping studies, or an individual brain. An example of a group intensity-averaged target is the MNI-305 brain that was created by averaging MR images from 305 young, normal subjects (Evans *et al.*, 1996), following global spatial normalization to a Talairach-like brain space (Talairach and Tournoux, 1988). For global spatial normalization, where feature matching primarily involves the brain location, size, and orientation, such an average brain

target is advantageous because it avoids spatial biases that can arise when using an individual brain (Woods, 1996; Lancaster *et al.*, 1999). For high-resolution, regional spatial normalization, an intensity-averaged target brain derived using global spatial normalization is not adequate, because feature matching must be extended to the limiting resolution of the brain images. To deal with this problem, Holmes *et al.* (1998) created a high-resolution, high-signal-to-noise-ratio MRI brain volume—the ICBM high-resolution brain template (HRBT). Twenty-seven high-resolution T1-weighted volumes (7 at 0.78 mm^3 and 20 at 1.0 mm^3) were acquired from a single subject (the author) on a Philips 1.5 Tesla MRI scanner. These 3-D image volumes were automatically registered to a common stereotaxic space in which they were subsampled and intensity averaged. The effect of intensity averaging of 27 volumes resulted in a gain of approximately 5 in the signal-to-noise ratio. As a result, fine anatomical details, such as thalamic subnuclei and the gray bridges between the caudate and the putamen, were well defined. Due to its excellent contrast and signal-to-noise ratio, this brain is currently used as a target for regional spatial normalization in many laboratories (Montreal Neurological Institute, UCLA Laboratory of Neuro Imaging, etc.). Also, many regions of this brain such as cerebellum (Schmahmann *et al.*, 1999), limbic system, ventricular system, hypothalamus (Toga and Thompson, 2001) have been manually segmented and labeled.

The HRBT provides excellent resolution and contrast detail; however, when selected as a target it will inevitably lead to a bias in the quality of regional spatial normalization due to anatomical features that are unique to this brain.

In Kochunov *et al.* (2001), methods were developed for defining, constructing, and evaluating a “minimal deformation target” (MDT) brain for multisubject studies based on analysis of the entire group. The goal was to provide a procedure that would create a standard, reproducible target brain based on commonality of features in a group of brain images. This research was based on the work performed by Grenander and Miller (1998), who first formalized the concept of an “average geometry target” as opposed to an intensity-averaged target. The MDT brain was defined to be the brain that minimizes deformation between the target and all the brains in a study. The need for minimal deformation is based on the fact that a displacement field is limited by continuity constraints in the amount of deformation that it can store (Kochunov *et al.*, 2000). Also, the average geometry of the target helps to avoid local minima during warping as the template is geometrically closer to all the brains (Grenander and Miller, 1998). The MDT optimization of the target brain leads to deformation fields for a group of brains with significantly reduced average displacement. Kochunov *et al.* (2001) also showed that warping individual brains to

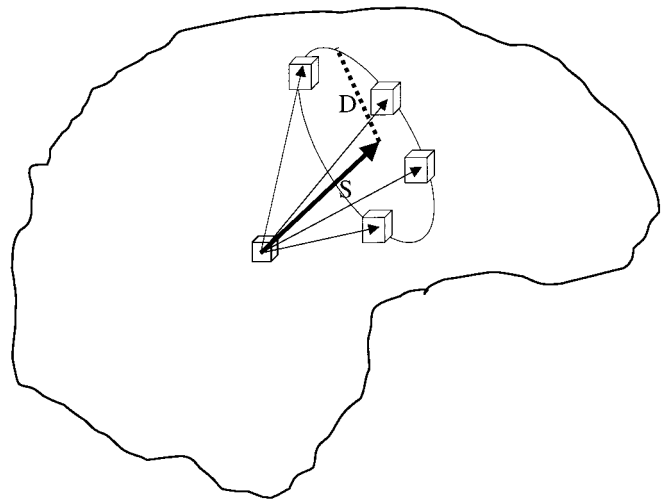


FIG. 1. A set of deformation vectors, pointing from a single voxel in the target brain to corresponding locations in a set of brains is shown. An average displacement vector S (boldface arrow) can be used to directly transform this voxel into its central (minimal deformation target) location, and dispersion vector D (dotted line) can be used to estimate variability of the deformation vectors about this optimal site.

the target brain that required the least amount of deformation for the group provided better feature matching as judged by an independent multiscale cross-correlation analysis.

An MDT target brain is obtained as follows: after global spatial normalization, a prospective target brain is warped to each brain in the study. The displacement fields (DFs), 3-D arrays of displacement vectors stored in each element, one per voxel, were saved and analyzed. The displacement vectors of each DF point from the target brain voxels to the corresponding locations in each source brain (Fig. 1). The set of displacement vectors, pointing from a single voxel in the target brain to corresponding locations in the set of source brains, mathematically describe the transformation of a target brain voxel into the collective brain space. An optimal target site was proposed as the geometrical centroid of the set of corresponding locations for each voxel. Averaging the set of DFs results in a DF that is used to directly transform the test brain into the MDT brain for the set (Fig. 1, boldfaced vector). The standard deviation of displacement vectors—the dispersion distance from the MDT brain site to corresponding locations (Fig. 1, dotted vector)—can be used to judge the agreement among brain images in this anatomical region. An empirical scoring function—“target quality score” (TQS) based on the product of the average displacement and the dispersion distance—was developed in Kochunov *et al.* (2001). The brain with the lowest TQS was declared the “best individual target” (BIT) brain.

Based on methods described in Kochunov *et al.* (2001), two strategies for selecting a target brain can

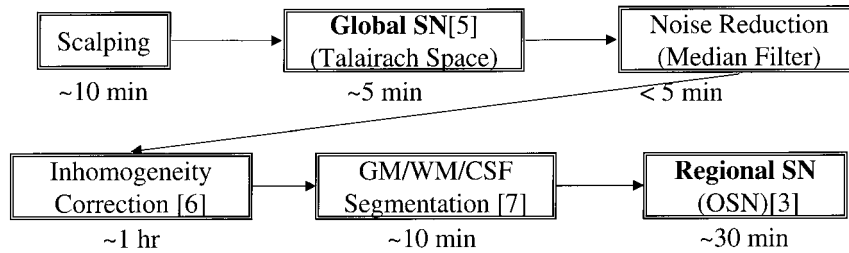


FIG. 2. The processing stream for global and regional spatial normalization (times for SUN Ultra-30, 250 MHz).

be proposed. First, the BIT brain can be reliably identified and optimized. Second, the total deformation magnitude of a well-established target brain can be minimized for a group of subjects. While the second strategy will not yield the best possible target for the group (as judged by the correlation analysis) it can be used to geometrically optimize a well-developed target brain such as the HRBT, where many anatomical structures are already manually segmented and labeled. The objective of this study was to evaluate the improvement in spatial normalization using the group-optimized HRBT.

MATERIALS AND METHODS

Subject Selection

Twenty-seven T1-weighted anatomical 3-D MRI brain images from three different labs (UCLA, MNI, and UTHSCSA) were selected from a group of healthy right-handed volunteers in the ICBM project (Mazziotta *et al.*, 1995). The subject population consisted of 14 males and 13 females. Twenty-five subjects were right-handed. Subjects ranged in age from 19 to 34 years with the average age of 24.8 ± 4.2 years.

Processing

The processing scheme is diagrammed in Fig. 2. Automated procedures were used to remove the skull tissues and cerebellum (scalping). All brain images were globally spatially normalized to the Talairach template using the Convex Hull software (Lancaster *et al.*, 1999; <http://ric.uthscsa.edu/projects>).

MR image intensity inhomogeneity was corrected using a bias-field analysis method developed by Styner *et al.* (2000). A fuzzy-classifier anatomical segmentation method (Herndon *et al.*, 1998) was used to segment images into white matter (WM), gray matter (GM), and cerebrospinal fluid (CSF). Anatomical templates (Kochunov *et al.*, 2000) were created by magnitude coding the tissue classes.

The optimized HRBT was obtained as follows: (1) the original HRBT was regionally spatially transformed with OSN to match each image in the study; (2) the resulting DF provided the set of displacement vectors,

pointing from a single voxel in the HRBT to corresponding locations in the set of source brains; and (3) the average vector for each voxel of the HRBT (Fig. 1) was used to transform this voxel into an optimal position in the collective brain space (Kochunov *et al.*, 2001).

Analysis

The optimized and original HRBTs were evaluated as the targets for regional spatial normalization. Each of the source images was warped to both the original and the optimized CH target brains, and the quality of match was evaluated for each of two groups. The WM/GM tissue mismatch for the right and left hemispheres was calculated for the target and source brains before and after OSN processing. The transformed source-to-target matching quality was evaluated using the multiscale cross-correlation analysis. The correlation analysis was introduced in Kochunov *et al.* (2001) to measure the spatial likeness between the source and the target images at varying scales. During the OSN feature-matching process (Kochunov *et al.*, 2000), a target dominant feature is identified as either WM, GM, CSF, or empty space in each octant. The average-per-octant cross-correlation coefficient (R) between target dominant tissue types in regionally transformed and target brains was calculated to assess the quality of match. This coefficient is an indicator of geometrical/anatomical similarity ($R \approx 1$) or difference (low R) between transformed and target brains. R is calculated at varying scales from large octants (128^3) at step 1 to small octants (2^3) at step 7 for the multiscale regional spatial transformation of OSN.

RESULTS

The optimized HRBT differed spatially from the original HRBT in several areas (Fig. 3). This 3-D view shows the regional nature of spatial changes due to the optimization process. The largest region affected by optimization was toward the dorsal surface of the brain, regions surrounding the central sulcus. The right superior precentral and postcentral gyri were moved anteriorly with an average displacement of about 6.5 mm; the same areas on the left side had

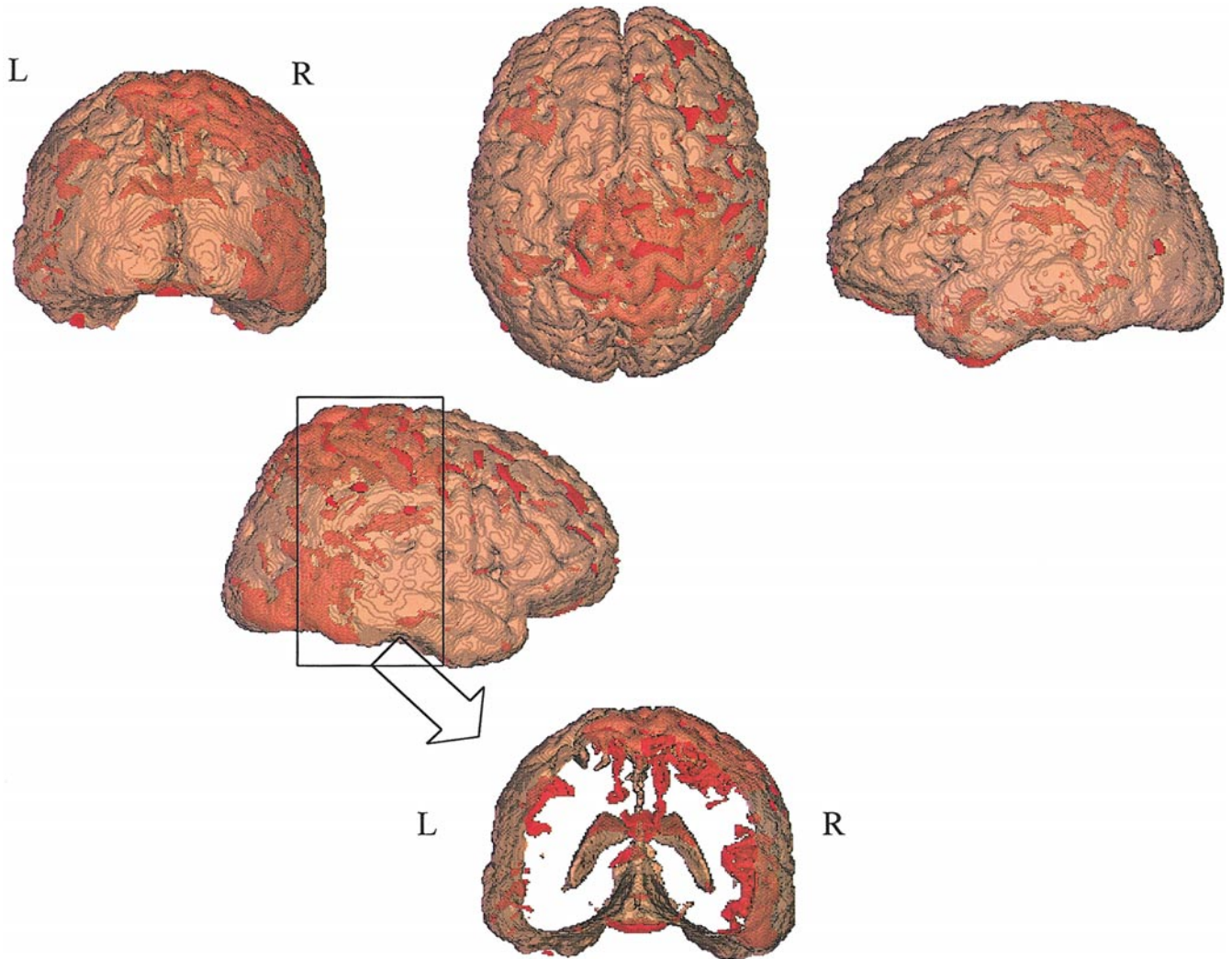


FIG. 3. Surface rendered views of optimized HRBT. Red indicates areas changed by optimization. Inset provides an internal view of changes.

average displacement of less than 2 mm. The standard deviation among the displacement vectors in the upper 20 mm of the precentral and postcentral gyri was 3.4 ± 2.4 mm on the left vs 2.5 ± 1.9 mm on the right (not significant at $P < 0.05$). Also the average coefficient of variation (displacement/SD) was significantly higher ($P < 0.05$) on the right (1.12 ± 0.34) than on the left (0.42 ± 0.32). Other changes included sizeable regions in the right inferior occipital/temporal lobes, lateral ventricles, and inferior frontal lobe.

The average GM matching error when the original HRBT was used as a target was $\sim 20\%$ following global SN and was reduced to about 9% following regional SN (Table 1). The optimization process produced mismatch that was about 8% (Table 1). The greatest mismatch improvement was on the right side of the brain, consistent with more optimization on the right side. The GM mismatch error was $\sim 8\%$ on the left and right following fitting to the optimized HRBT. The average

WM mismatch was about 12% following global SN and was reduced to $\sim 7\%$ following OSN processing. When images were warped to the optimized HRBT the WM mismatch following OSN processing was reduced to less than 6%.

TABLE 1

Percent Gray Matter (GM) and White Matter (WM) Boundary Mismatch for 27 Brains after Matching to the Original HRBT (A) and the Optimized HRBT (B)

SN method	Left GM	Right GM	Left WM	Right WM
A				
GSN	17.9 ± 2.5	18.2 ± 2.3	12.5 ± 1.7	12.4 ± 1.6
OSN	9.2 ± 1.5	9.12 ± 1.3	6.7 ± 1.14	6.6 ± 1.1
B				
GSN	17.0 ± 2.0	16.4 ± 1.8	11.9 ± 1.4	11.5 ± 1.14
OSN	8.4 ± 1.4	8.2 ± 1.1	6.3 ± 1.0	5.9 ± 0.8

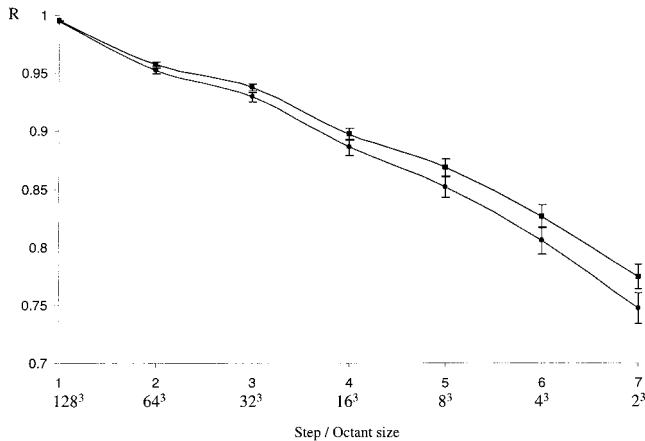


FIGURE 4

The plots of transformed-to-target brain image average cross-correlation (Fig. 4) show that the Rs improve following warping to the optimized HRBT (top curve) especially at smaller scales (steps 5–7), indicating better anatomical match among the group of brains. The average GM spatial cross-correlation coefficients, calculated in the areas where the two templates were different (red areas in Fig. 3), are shown in Table 2. Warping to the optimized HRBT resulted in significantly higher correlation ($P < 0.05$) in the areas affected by optimization compared to the original HRBT.

DISCUSSION AND CONCLUSION

A novel method to reliably identify and optimize the BIT brain for a group of 3-D MRI brain images (Kochunov *et al.*, 2001) was used to make the HRBT a better regional SN target. Using a well-developed target such as the HRBT, where many regions are already manually segmented and labeled, provides a practical advantage over selecting an individual target brain since manual segmentation is very time consuming.

The MDT displacement field provides the values for the mean displacement vector (the boldfaced vector, Fig. 1) for each voxel of the target brain and the standard deviation or spatial spread about the mean (the dotted vector, Fig. 1). The mean displacement vector indicates the distance from the target brain to the mean corresponding location for the group. The standard deviation about the mean location is a measure of the spatial consistency of this anatomical location within the group. Higher spatial spread indicates significant variation in the location of this anatomical region among the brains in the group. This situation was observed at the precentral and postcentral gyri on the left side. The more complex anatomy and higher degree of nonhomology in the dominant hemisphere is believed to be the cause of higher spatial spread on the left side. This is supported by the findings in the study

of the degree of cortical folding—gyrification index (GI)—performed by Zilles *et al.* (1997), which reports GI being significantly higher for the left hemisphere.

The higher displacements on the right side resulted in a 6.5-mm anterior move of the dorsal part of the right central sulcus in the optimized HRBT. Thompson *et al.* (1998, 2001) reported that the superior portion of the average right central sulcus was located about 8 mm more anterior relative to that of the left central sulcus. That asymmetry was observed in the normal and diseased populations of subjects. The dorsal part of the right central sulcus of the HRBT was originally located at the about the same level as the left central sulcus but was moved to match the “middle of the group” by the optimization process.

The lower spatial spread of right precentral and postcentral gyri among the source brains can be attributed to more similarities among the sulcal features. This assumption is supported by the prior studies of sulcal variability of precentral, central, and postcentral sulci in a group of 10 subjects (Kochunov *et al.*, 2000). Following OSN processing, the central sulcus on the right side had significantly less spatial variability than that on the left side even though the sulcal variability on the right was slightly higher than that on the left following the global SN. Similar findings were also reported by Missir *et al.* (1989), Zilles *et al.* (1997), and Le Goualher *et al.* (2000).

Ideally, the MDT optimization should position homologous locations in the target brain to central locations, characteristic of the group. This is not achievable for biological and technical reasons. While many anatomical features are present in all brains, some are present in most brains and others are individually unique (e.g., some sulci created during secondary gyration). Thus, a principal goal of target brain optimization, reduction of individual features in the target brain, is impeded by using a single brain with many individual features. Previous work demonstrated how selecting a highly unique individual brain could be avoided, but that was clearly not the goal in MDT optimization of the HRBT brain. Currently, technical limitations due to failure to extract and match desired anatomical features are believed to be dominate biological issues. While the matching methodology (cross-correlation) is adequate, the feature extraction, via

TABLE 2

Average GM Spatial Correlation Coefficients in the Areas Affected by the Optimization Process after Matching to the Optimized and Original HRBT Targets

Octant size	Optimized colin brain	Original colin brain
4 ³	0.63 ± 0.023	0.52 ± 0.026
2 ³	0.57 ± 0.028	0.48 ± 0.029

anatomical segmentation, still needs improvement. Better image quality and better segmentation methods should improve the extraction of anatomical features. With sufficient technical improvements, the biological limitations of the optimization procedure will become the main limitation.

REFERENCES

- Ashburner, J., and Friston, K. 1997. Multimodal image coregistration and partitioning—a unified framework. *NeuroImage* 6: 209–217.
- Ashburner, J., and Friston, K. J. 1999. Nonlinear spatial normalization using basis functions. *Human Brain Mapp.* 7: 254–266.
- Collins, D., Holmes, C., Peters, T., and Evans, A. 1995. Automatic 3-D model-based neuroanatomical segmentation. *Human Brain Mapp.* 3: 190–208.
- Evans, A., Collins, D., and Holmes, C. 1996. Computational approaches to quantifying human neuroanatomical variability. In *Brain Mapping: The Methods* (A. Toga and J. Mazziotta, Eds.), pp. 343–361. Academic Press, San Diego.
- Fox, P., Perlmutter, J., and Raichle, M. 1985. A stereotactic method of anatomical localization for positron emission tomography. *J. Comput. Assist. Tomogr.* 9: 141–153.
- Fox, P. 1995. Spatial normalization origins: Objectives, applications, and alternatives. *Human Brain Mapp.* 3: 161–164.
- Grenander, U., and Michael, M. 1998. Computational anatomy: An emerging discipline. *Q. Appl. Math.* LVI: 617–694.
- Herndon, R. C., Lancaster, J. L., Giedd, J., and Fox, P. T. 1998. Quantification of white matter and gray matter volumes from 3-D magnetic resonance volume studies using fuzzy classifiers. *J. Magn. Reson. Imag.* 8: 1097–1105.
- Holmes, C. J., Hoge, R., Collins, L., Woods, R., Toga, A. W., and Evans, A. C. 1998. Enhancement of MR images using registration for signal averaging. *J. Comput. Assist. Tomogr.* 22: 324–333.
- Kochunov, P., Lancaster, J., and Fox, P. 1999. Accurate high-speed spatial normalization using an octree method. *NeuroImage* 10: 724–737.
- Kochunov, P., Lancaster, J., Thompson, P., Boyer, A., Hardies, J., and Fox, P. 2000. Evaluation of octree regional spatial normalization method for regional anatomical matching. *Human Brain Mapp.* 11: 193–206.
- Kochunov, P., Lancaster, J., Thompson, P., et al. 2001. Regional spatial normalization: Towards the optimal target. *J. Comput. Assist. Tomogr.* 25: 805–816.
- Lancaster, J. L., Glass, T. G., Lankipalli, B. R., Downs, H., Mayberg, H., and Fox, P. T. 1995. A modality-independent approach to spatial normalization of tomographic images of the human brain. *Human Brain Mapp.* 3: 209–223.
- Lancaster, J. L., Rainey, L. H., Summerlin, J. L., Freitas, C. S., Fox, P. T., Evans, A. C., Toga, A. W., and Mazziotta, J. C. 1997. Automated labeling of the human brain: A preliminary report on the development and evaluation of a forward-transform method. *Human Brain Mapp.* 5: 238–242.
- Lancaster, J. L., Fox, P. T., Downs, H., et al. 1999. Global spatial normalization of the human brain using convex hulls. *J. Nucl. Med.* 40: 942–955.
- Lancaster, J. L., Woldorff, M. G., Parsons, L. M., Liotti, M., Freitas, C. S., Rainey, L., Kochunov, P. V., Nickerson, D., Mikiten, S. A., and Fox, P. T. 2000. Automated Talairach Atlas labels for functional brain mapping. *Human Brain Mapp.* 10: 120–131.
- Le Goualher, G., Argenti, A. M., Duyme, M., Baare, W. F., Hulshoff Pol, H. E., Boomsma, D. I., Zouaoui, A., Barillot, C., and Evans, A. C. 2000. Statistical sulcal shape comparisons: Application to the detection of genetic encoding of the central sulcus shape. *NeuroImage* 11: 564–574.
- Mazziotta, J. C., Toga, A. W., Evans, A., et al. 1995. A probabilistic atlas of the human brain: Theory and rationale for its development. *NeuroImage* 2: 89–101.
- Miller, M., Christensen, G., Amit, Y., and Grenander, U. 1993. Mathematical textbook of deformable neuroanatomies. *Proc. Natl. Acad. Sci. USA* 90: 11944–11948.
- Missir, O., Dutheil-Desclercs, C., Meder, J. F., Musolino, A., and Frey, D. 1989. Central sulcus patterns at MRI. *J. Neuroradiol.* 16: 133–144.
- Schmahmann, J. D., Doyon, J., McDonald, D., Holmes, C., Lavoie, K., Hurwitz, A. S., Kabani, N., Toga, A., Evans, A., and Petrides, M. 1999. Three-dimensional MRI atlas of the human cerebellum in proportional stereotaxic space. *NeuroImage* 10: 233–260.
- Styner, M., Brechbühler, C., Székely, G., and Gerig, G. 2000. Parametric estimate of intensity inhomogeneities applied to MRI. *IEEE Trans. Med. Imag.* 19: 153–165.
- Talairach, J., and Tournoux, P. 1988. *Co-Planar Stereotaxic Atlas of the Human Brain*. Thieme, New York.
- Thompson, P. M., Moussai, J., Zohoori, S., Goldkorn, A., Khan, A. A., Mega, M. S., Small, G. W., Cummings, J. L., and Toga, A. W. 1998. Cortical variability and asymmetry in normal aging and Alzheimer's disease. *Cereb. Cortex* 8: 492–509.
- Thompson, P. M., Mega, M. S., Woods, R. P., Zoumalan, C. I., Lindshield, C. J., Blanton, R. E., Moussai, J., Holmes, C. J., Cummings, J. L., and Toga, A. W. 2001. Cortical change in Alzheimer's disease detected with a disease-specific population-based brain atlas. *Cereb. Cortex* 11: 1–16.
- Toga, A. W., and Thompson, P. M. 2001. Maps of the brain. *Anat. Rec.* 265: 37–53.
- Woods, R. P., Mazziotta, J. C., and Cherry, S. R. 1993. MRI–PET registration with automated algorithm. *J. Comput. Assist. Tomogr.* 17: 536–546.
- Woods, R. P. 1996. Correlation of brain structure and function. In *Brain Mapping: The Methods* (A. W. Toga and J. C. Mazziotta, Eds.), pp. 313–342. Academic Press, San Diego.
- Zilles, K., Schleicher, A., Langemann, C., Amunts, K., Morosan, P., Palomero-Gallagher, P., Schormann, T., Mohlberg, H., Bürgel, U., Steinmetz, H., Schlag, G., and Roland, P. 1997. Quantitative analysis of sulci in the human cerebral cortex: Development, regional heterogeneity, gender difference, asymmetry, intersubject variability and cortical architecture. *Human Brain Mapp.* 5: 218–221.